

Statistical Prediction of “Reasonable Worst-Case” Crosstalk in Cable Bundles

Meilin Wu, Daryl G. Beetner, *Senior Member, IEEE*, Todd H. Hubing, *Fellow, IEEE*, Haixin Ke, *Member, IEEE*, and Shishuang Sun, *Member, IEEE*

Abstract—Worst-case estimates of crosstalk in cable bundles are useful for flagging potential problems, but may also flag problems that only occur very rarely, due to the random variation of wire positions and other characteristics of the harness. Prediction of crosstalk that may realistically occur requires statistical methods. Monte Carlo simulation techniques are often used to account for statistical variation, but are time consuming and do not provide intuition toward the cause of, or solution to, problems. Here, we investigate prediction of the statistically “reasonable worst-case” crosstalk by forming probability distributions using inductance and capacitance parameters from a single harness cross section and using lumped-element approximations for crosstalk that account for strong coupling within the harness when the circuit is electrically small. The accuracy of this technique was evaluated through comparison to simulation results using the random displacement spline interpolation method for multiple random instantiations of several harness configurations. Tests were performed while varying the size of the bundle, its height above the return plane, the value of load impedances, and the presence of a return wire. The reasonable worst-case crosstalk was estimated within about 5 dB or less in each case.

Index Terms—Automotive, cable harness, crosstalk, multiconductor transmission lines, statistics.

I. INTRODUCTION

PREDICTING electromagnetic interference problems early in the design process is a significant challenge in many industries. Complex simulation tools have the potential to estimate interference very accurately, but significant time is required to enter design information and perform simulations, and results are not always easy to interpret. While the presence of a problem may be found with these tools, the problem’s cause or solution may not be obvious. Statistical variation of system parameters, like the random variation of wire position within a harness, adds to the challenge [1], [2]. Accounting for statistical variations using simulation models typically requires simulation of many possible design configurations to estimate

the range of interference problems. Worst-case analysis using lumped-element models provides rapid solutions at low frequencies with a clear indication of the parameters that may cause a problem [3], though solutions based on worst-case analyses may be too conservative and overestimate interference that is statistically *likely* to occur [4]. Methods are needed to quickly estimate statistically reasonable estimates of crosstalk in a way that provides a clear link between the observed interference and the system characteristics that cause that interference.

Several methods have been developed for estimating the statistical variation of crosstalk in cable harness bundles. Efforts to develop a closed-form estimate of statistical variation have so far been unsuccessful, requiring at least some numerical intervention to generate results [5]. Most solutions rely on Monte Carlo simulations of multiple harness configurations. For example, Ciccolella and Canavero use Monte Carlo methods to estimate a cumulative distribution function for crosstalk through numerical solution of multiconductor transmission-line equations [6]. Position is varied by segmenting the harness along its length and choosing a random position for each wire within each segment. Sun *et al.* develop a similar method called the random displacement spline interpolation (RDSI) method that allows for smooth variation of the position of the wires from one segment to another [7]. Both methods rely on the numerical solution of many harness configurations, thus requiring significant computational effort.

Another method for dealing with the statistical variation of crosstalk that promises to significantly reduce computational effort was proposed by Bellan and Pignari [8]. The method estimates the statistical variation of crosstalk using lumped two-wire models for crosstalk and the statistical variation of inductance or capacitance within a single harness cross section. This method works well at low frequencies (e.g., 1 kHz), where weak coupling may be assumed. This method was extended in [9] to work at frequencies where weak coupling does not apply by proposing simple limits to estimate the “reasonable worst-case crosstalk” (e.g., the worst crosstalk that would occur in 99% of configurations).

Here, we further extend the work proposed in [8] and [9] to develop closed-form estimates of the statistically reasonable worst-case crosstalk when the harness is electrically small, but weak coupling cannot be assumed, and demonstrate the applicability of the model over a wide frequency range and over many harness configurations. The following paragraphs will explain the theory behind the approach and will show the ability of the method to predict the reasonable worst-case crosstalk through comparison to simulations using the RDSI method. Multiple

Manuscript received September 4, 2008; revised May 6, 2009. First published August 11, 2009; current version published August 21, 2009.

M. Wu was with Missouri University of Science and Technology (formerly University of Missouri-Rolla), Rolla, MO 65409 USA. He is now with Amphenol-TCS, Nashua, NH 03062 USA (e-mail: mwqz2@mst.edu).

D. G. Beetner is with Missouri University of Science and Technology (formerly University of Missouri-Rolla), Rolla, MO 65409 USA (e-mail: daryl1@mst.edu).

T. H. Hubing and H. Ke are with Clemson University, Clemson, SC 29635 USA (e-mail: t.hubing@ieee.org; hxkeucl@clemson.edu).

S. Sun is with Altera Corporation, San Jose, CA 95134 USA (e-mail: ssun@altera.com).

Color versions of one or more of the figures in this paper are available online at <http://ieeexplore.ieee.org>.

Digital Object Identifier 10.1109/TEM.2009.2026740

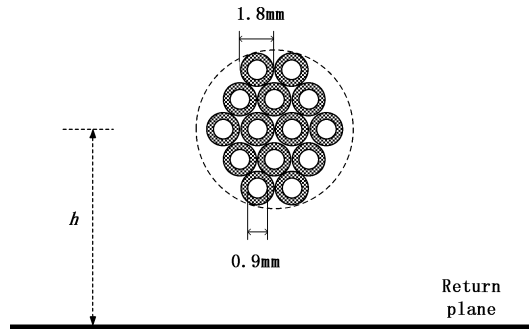


Fig. 1. Cross section of a 14-wire harness.

harness configurations will be explored, including the impact of high and low termination impedances, the use of return wires, the influence of bundle height above the return plane, and the influence of the number of wires in the harness.

II. ESTIMATION OF VARIATION OF INDUCTANCE AND CAPACITANCE

Lumped-element models can be used to estimate crosstalk at low frequencies, where circuits are electrically small, given the self-inductance and mutual inductance, and capacitance among circuits. Estimation of crosstalk in harnesses is difficult because the position of a wire within the harness is often unknown, the position changes along the wire length (often associated with bundle “twist”), and the influence of other wires in the harness cannot necessarily be ignored when calculating crosstalk between a particular culprit and victim.

A common method for dealing with the random position of wires within the harness is to calculate values of inductance and capacitance for a specific, fixed, harness cross section, to assume that this cross section reasonably approximates any cross section of the harness, and to account for twist by splitting the harness into segments and by giving circuits a new, random position within each segment [6]–[8]. Crosstalk is calculated from the inductance and capacitance parameters of the harness segments. The rate that wires change along the length of the wire (i.e., the amount of twist) is controlled by the number of segments. Here, we use this same approach to first estimate the statistical variation of the self-inductance and mutual inductance, and capacitance within the harness, and then to estimate the crosstalk between harness circuits.

An example of a bundle cross section used in this study is shown in Fig. 1. This bundle consists of fourteen 20-gauge copper wires separated by the thickness of the polyvinyl chloride (PVC) insulation, which was set equal to the radius of the wires. The height of the center of the bundle from the return plane was typically 2 cm, though experiments were also performed with the harness lying directly on the return plane. Matrices [10] describing the per-unit-length self-inductance and mutual inductance within the harness cross section were found using the 2-D electromagnetic modeling tool, Ansoft Maxwell 2-D Extractor. The wire for a particular circuit was assumed to take on any one position within the harness with equal probability. To simplify the analysis, the position of a wire within one harness

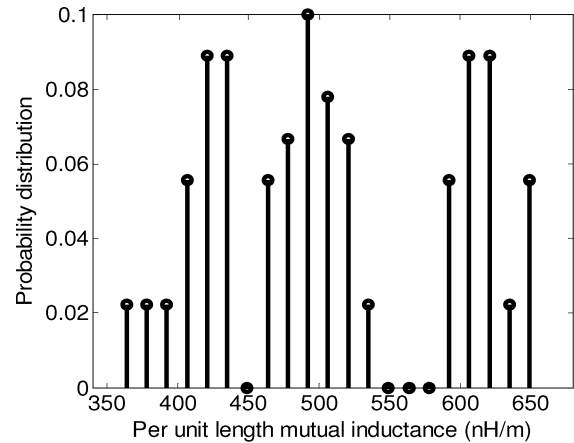


Fig. 2. Probability distribution for per-unit-length mutual inductance for a single segment of a harness containing fourteen 20-gauge wires 2 cm above a return plane.

segment was assumed to be independent of its position in any other segment.

The statistical distribution of the per-unit-length inductance or capacitance from one wire to any other wire within the harness or to the return plane can be determined from the inductance and capacitance matrices calculated using a 2-D modeling tool. The probability distribution for self-inductance with respect to the return plane is found from the number of occurrences of a value along the main diagonal of the inductance matrix. The probability distribution for mutual inductance is found from the upper triangle of the matrix. Probability distributions for self-capacitance and mutual capacitance can be found in a similar manner.

Crosstalk is calculated from the average per-unit-length inductance and capacitance along the harness, and from the harness length. The average per-unit-length inductance or capacitance is a weighted sum of the per-unit-length inductance or capacitance for each segment. Since these are random quantities, the average per-unit-length inductance or capacitance is a weighted sum of random variables. As each random variable is independent and has the same probability distribution, say $f_s(x)$, the probability distribution for the average per-unit-length inductance or capacitance for the harness, say $f_h(x)$, is given by a convolution of probability distributions for the segments. For example, for two segments of equal length, the probability distribution of the average per-unit-length inductance or capacitance of the harness is given by [11]

$$f_h(x) = \int_{-\infty}^{\infty} f_s(2x - y)f_s(y)dy. \quad (1)$$

More than two segments would require a series of similar convolutions.

Typical probability distributions generated using this technique are illustrated in Figs. 2–5. Plots were generated using the harness cross section shown in Fig. 1 with 14 wires and a height h of 2 cm above the return plane. Fig. 2 shows the probability distribution for the per-unit-length mutual inductance generated from the upper triangle of the inductance matrix. Fig. 3

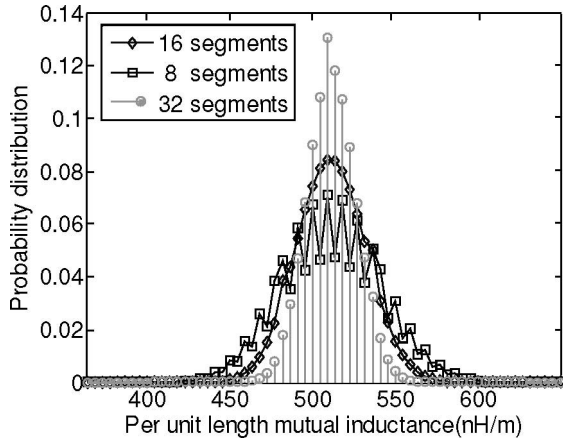


Fig. 3. Probability distribution of “effective” per-unit-length mutual inductance for a wiring harness containing fourteen 20-gauge wires 2 cm above a return plane.

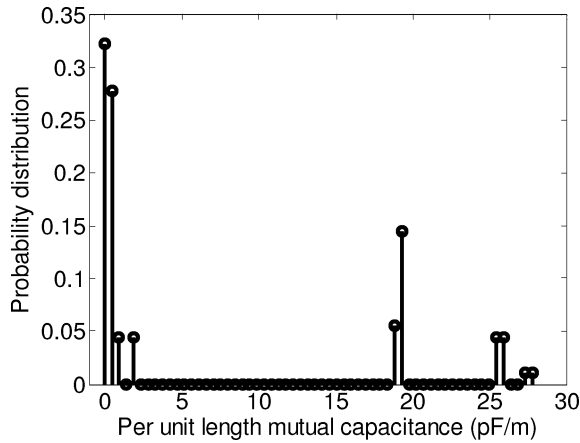


Fig. 4. Probability distribution of per-unit-length mutual capacitance for a single segment of a harness containing fourteen 20-gauge wires 2 cm above a return plane.

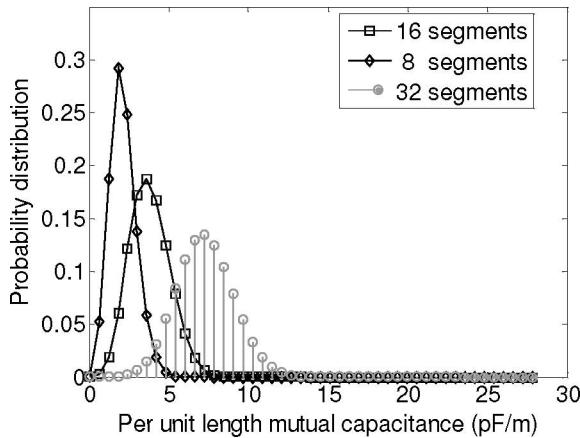


Fig. 5. Probability distribution of the “effective” per-unit-length mutual capacitance for a wiring harness containing fourteen 20-gauge wires 2 cm above a return plane.

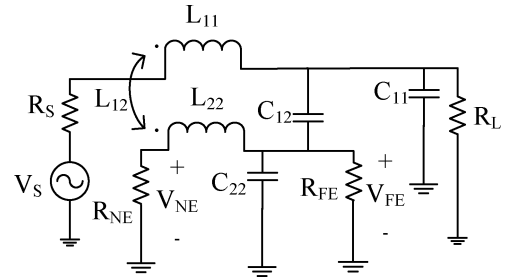


Fig. 6. Low-frequency model for crosstalk.

shows the probability distribution for the average or “effective” per-unit-length mutual inductance over the entire harness after breaking the harness into 8, 16, or 32 segments, and assuming a new, random position of each wire for each segment. The nearly uniform nature of the probability distribution for a single segment causes the probability distribution for multiple segments to get progressively narrower as the number of segments increases. Figs. 4 and 5 show the probability distributions for the per-unit-length mutual capacitances for a single segment and for 8, 16, and 32 segments. In this case, the probability distribution for a single segment is asymmetrical, as very small values of mutual capacitance are much more likely than large values, and the probability distribution envelope becomes wider and the median value moves to the right (i.e., to larger values of capacitance) as additional segments are added.

III. ESTIMATION OF “REASONABLE WORST-CASE” CROSSTALK

At low frequencies where the harness is electrically small, crosstalk can be estimated using simple lumped-element equations with information about only the culprit and victim circuits, and the mutual inductance or capacitance between them [8], [9]. A two-wire-harness model for crosstalk in this case is shown in Fig. 6. When inductive coupling dominates and weak coupling applies (i.e., the voltage/current induced in a victim only weakly influences the voltage/current in the culprit), mutual capacitance can be ignored and the far-end inductive crosstalk is given approximately by

$$x_{\text{talk}_{\text{ind}}} = \frac{V_{\text{FE_IND}}}{V_S} \approx \frac{-j\omega L_{12}}{(R_S + R_L + j\omega L_{11})} \frac{R_{\text{FE}}}{(R_{\text{NE}} + R_{\text{FE}} + j\omega L_{22})} \quad (2)$$

where self-capacitance is ignored assuming that $(R_{\text{NE}}//R_{\text{FE}}) \ll 1/j\omega C_{11}$ or $1/j\omega C_{22}$. When capacitive coupling dominates and weak coupling applies, mutual inductance can be ignored and

$$x_{\text{talk}_{\text{cap}}} = \frac{V_{\text{FE_CAP}}}{V_S} \approx \frac{R_L}{R_S + j\omega L_{11} + R_L} (R_{\text{NE}}//R_{\text{FE}}) j\omega C_{12} \quad (3)$$

where it is assumed that the influence of self-inductance in the victim circuit is negligible and that

$$(R_{\text{NE}}//R_{\text{FE}}) \ll 1/j\omega C_{11} \text{ or } 1/j\omega C_{22}.$$

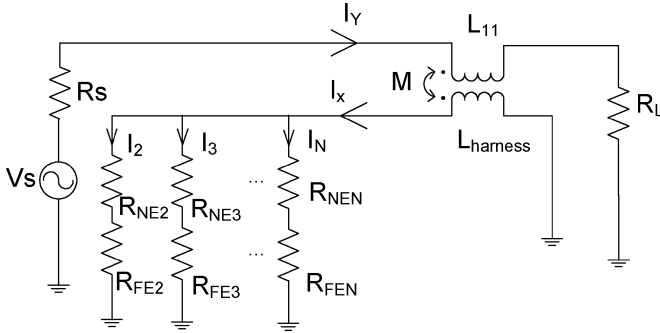


Fig. 7. Circuit model approximating strong inductive coupling.

Worst-case crosstalk among harness configurations can be estimated from the largest value of mutual capacitance or inductance, though this value of crosstalk may occur only very rarely. “Reasonable” worst-case crosstalk can be estimated from the largest values of mutual inductance or capacitance that will occur over a large percentage of harness configurations. For example, for the case shown in Fig. 3, the worst-case value of per-unit-length mutual inductance is about 650 nH/m; yet, in more than 99% of configurations, the worst effective mutual inductance over the length of the harness is less than 570 nH/m when wires change position 32 times over the harness length. A statistically reasonable estimate of worst-case inductive crosstalk (i.e., the worst crosstalk in 99% of configurations) could be found using a mutual inductance of 570 nH/m in crosstalk calculations.

At higher frequencies, the weak coupling assumption breaks down and the influence of the other circuits in a multiconductor harness must be taken into account [9]. This scenario can be approximated using the circuit in Fig. 7. When inductive coupling dominates, the main influence on crosstalk is the magnetic field through the “loop” associated with the harness. Each circuit in the harness contributes to this magnetic field. A culprit circuit will generate a magnetic flux through the harness “loop” that will cause a voltage drop across every other circuit in the harness. If one assumes that the harness is sufficiently high above the return plane and that the mutual inductance from the culprit to every other circuit in the harness is approximately the same, then a voltage drop of approximately $j\omega MI_y$ will be induced across each victim, where M is the mutual inductance between the culprit and each victim, and I_y is the current in the culprit. This voltage drop will create a (different) current in each victim that is inversely proportional to the total impedance in each circuit. These currents, in turn, will create additional magnetic flux that will further influence the voltage drop in each circuit, including the culprit. The total magnetic flux generated by the victims is associated with the net current through the victims. If one assumes that the victim circuits are sufficiently high above the return plane, and that their self-inductances and the mutual inductances between them are approximately equal, then the influence of the magnetic flux associated with the net current through the victims can be represented approximately using a single inductance for the harness L_{harness} . One can also think

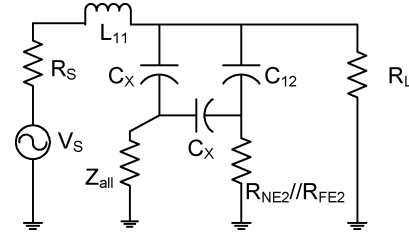


Fig. 8. Circuit model approximating strong capacitive coupling.

of L_{harness} as the common-mode inductance of the victim circuits. Using these approximations, the far-end crosstalk due to inductive coupling in the victim of interest (circuit 2) is given approximately by

$$x_{\text{talk}_{\text{ind}}} \approx - \left(\frac{R_{\text{FE}2}}{R_{\text{NE}2} + R_{\text{FE}2}} \right) \times \left(\frac{j\omega M Z}{(\omega M)^2 + (R_s + R_L + j\omega L_{11})(Z + j\omega L_{\text{harness}})} \right) \quad (4)$$

where Z is the effective impedance of the victim circuits, $Z = (R_{\text{NE}2} + R_{\text{FE}2}) || (R_{\text{NE}3} + R_{\text{FE}3}) || \dots || (R_{\text{NEN}} + R_{\text{FEN}})$, M is calculated from the net per-unit-length mutual inductance along the harness, $M = l_m \times \text{length}$, where l_m is the per-unit-length mutual inductance between the culprit and victim circuits, and “length” is the length of the harness. L_{11} can be approximated from the average per-unit-length self-inductance of all the circuits in the harness, $L_{11} = l_{s_{\text{avg}}} \times \text{length}$, where $l_{s_{\text{avg}}}$ is calculated from the average value of the main diagonal of the inductance matrix. The self-inductance of the harness L_{harness} can be approximated by the value of the mutual inductance M since both are related to the total flux through the harness loop. In (4), weak coupling is not assumed and the current in the culprit can be influenced by the victim circuits, as shown by the term $(\omega M)^2$ in the denominator of the equation.

A similar approximation can be made for capacitive coupling when weak coupling cannot be assumed. The victim circuits are again lumped together, as shown in Fig. 8. The model shows the mutual capacitance C_{12} from the culprit to the victim of interest (represented by resistance $R_{\text{NE}2} // R_{\text{FE}2}$). This part of the model is similar to Fig. 6 when L_{22} and C_{22} are ignored, as in (2). The model in Fig. 8 also represents the capacitive coupling from the culprit to all other circuits in the harness using the elements Z_{all} and C_x , where Z_{all} is the parallel impedance of all other circuits in the harness, $Z_{\text{all}} = R_{\text{NE}3} // R_{\text{FE}3} // \dots // R_{\text{NEN}} // R_{\text{FEN}}$, and C_x is the total capacitance to all other circuits in the harness and the return plane $C_x = C_{o_{\text{avg}}} - C_{12}$, where C_{12} is calculated from the per-unit-length mutual capacitance c_m , as found from the capacitance matrix, $C_{12} = c_m \times \text{length}$, and $C_{o_{\text{avg}}}$ is calculated from the average per-unit-length value of capacitance given on the main diagonal of the (Maxwell) capacitance matrix [10]. The capacitance to the return plane is assumed to be small compared to other values of capacitance and is ignored in this approximation. Self-inductance of the victim circuits was similarly ignored because it is rarely important for capacitive

coupling. Self-inductance of the culprit circuit was included since it may limit the voltage across the culprit, and thus, influence capacitive coupling.

The model in Fig. 8 was constructed to minimize the number of random variables in the circuit. While we do not know the values of mutual capacitance for specific circuits in Fig. 8, we do know the value of C_x once a value of C_{12} is given, and therefore, can simplify the statistics considerably by forming a model using C_x rather than individual capacitances. The premise behind Fig. 8 is that energy is coupled from the victim to all the circuits in the harness through some coupling capacitance. Some of this energy, depending on the impedances in the harness, will be coupled between the victims. While this model is approximate, there were three essential conditions that were considered in its construction. First is the case where the termination resistances of each circuit are sufficiently small that $1/j\omega C_{ij} \gg R_{NEi} || R_{FEi}$ for all circuits i and all $j > 1$. In this case, the crosstalk current drawn from the culprit circuit is relatively small, as determined by the mutual capacitance, and second-order coupling from one victim to another is negligible. This model will accurately predict crosstalk in this scenario. A second case of interest is where resistances are large, $1/j\omega C_{ij} \ll R_{NEi} || R_{FEi}$ for all circuits i and all $j > 1$. In this case, the circuits are strongly coupled, the current drawn from the culprit is approximately determined by the parallel equivalent of the victim terminations, $R_{NE2} // R_{FE2} // \dots // R_{NEi} // R_{FEi}$, and the voltage across each victim termination is approximately equal. This scenario is also accurately predicted by the model. A third case of interest is where the sum of coupling capacitances and resistances are approximately equal, i.e., where $1/j\omega C_{1i} + R_{NEi} || R_{FEi} \approx 1/j\omega C_{1j} + R_{NEj} || R_{FEj}$ for $i, j > 2$. Since they are nearly equal, the parallel combination of these resistances and capacitances is given by approximately $1/j\omega C_x + Z_{all}$. Some of the voltage dropped across the termination Z_{all} will also be coupled back to circuit 2, the victim of interest. Since the voltage is approximately the same across all terminations, $R_{NEi} || R_{FEi}$ for $i > 2$, the coupling capacitances to circuit 2 can be considered in parallel, so that the total coupling capacitance is given by the sum of these capacitances, i.e., by C_x . This scenario is also accurately modeled by the circuit. Other scenarios may not be modeled as accurately, but should be reasonably close, especially considering that coupling among the victim circuits is not typically a large contributor to the noise voltage seen on a particular victim.

Based on this model, the far-end capacitive crosstalk in the victim of interest (circuit #2) is approximately, as in (5), shown at the bottom of the page, where $Z_x \cong R_L // ((1/j\omega C_{o_avg}) + R_{NE2} // R_{FE2} // Z_{all})$.

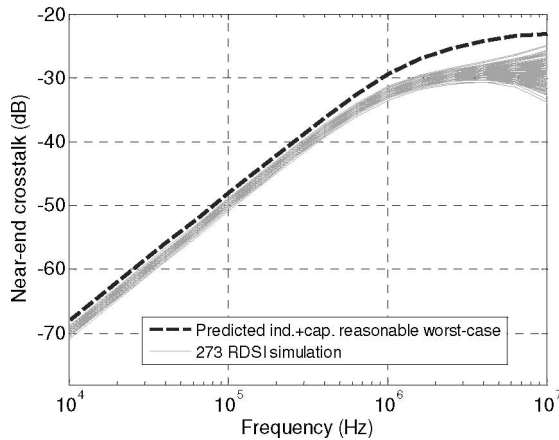
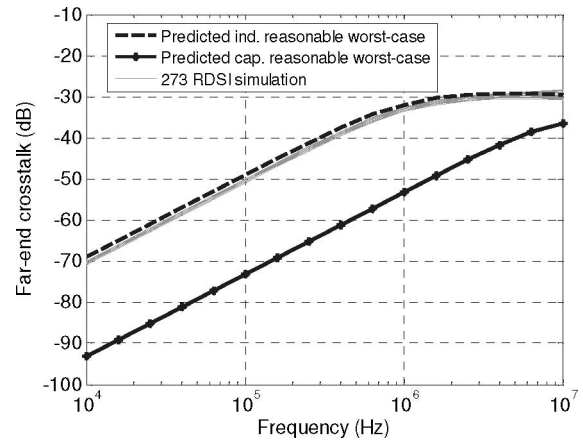
The reasonable worst-case inductive or capacitive crosstalk can be estimated from (4) or (5) using the reasonable worst-case values of mutual inductance or capacitance (e.g., using 570 nH/m for the configuration in Fig. 3). Using these values al-

lows one to calculate the reasonable worst-case crosstalk due to either inductive or capacitive coupling, but not necessarily due to both, since large values of mutual capacitance may not occur for the same configurations that cause large values of mutual inductance. Since the joint relationship between inductive and capacitive couplings is complicated, and typically, either one or the other dominates, a simple heuristic based on a two-wire-harness model was used here to approximate the total crosstalk. At the near end, where inductive and capacitive crosstalks are in phase, the magnitude of the total crosstalk is a sum of the magnitude of the capacitive and inductive crosstalks. In this case, the reasonable worst-case crosstalk was approximated as the sum of crosstalk calculated using (1) and (2). This approximation should predict the reasonable worst-case crosstalk within 6 dB. When both capacitive and inductive crosstalks peak at the same time, this sum will accurately predict the overall crosstalk at the near end. If the reasonable worst-case crosstalk occurs when inductive coupling is zero, or *vice versa*, then a sum of the reasonable worst-case inductive and capacitive couplings will be not more than 6 dB higher than the actual crosstalk. At the far end, where inductive and capacitive crosstalks are out of phase by 180° , the total crosstalk was approximated as the larger of (4) and (5). When the reasonable worst-case inductive and capacitive couplings occur at the same time, this approximation will overestimate crosstalk since the two will cancel. If the reasonable worst-case inductive coupling occurs when capacitive coupling is zero, or *vice versa*, this approximation will accurately predict the actual crosstalk. While this approximation may overestimate the far-end crosstalk in some cases, it should not underestimate crosstalk and should be reasonably close to the correct value when either inductive or capacitive crosstalk dominates.

IV. APPLICATION OF THE METHOD

The proposed method of estimating reasonable worst-case crosstalk was tested by applying it to several test configurations and comparing results to crosstalk calculated using the RDSI algorithm [7]. The RDSI algorithm has previously been shown to produce results that closely match experimental data [7]. Both the RDSI algorithm and the reasonable worst-case estimate were based on the numerical solution of L and C matrices using Ansoft Maxwell 2-D Extractor for a harness cross section like the one shown in Fig. 1. The RDSI algorithm then used Monte Carlo methods and HSPICE simulations to estimate the total crosstalk (inductive + capacitive) for several possible wire position configurations within the harness. The reasonable worst-case crosstalk was estimated using (4) and (5), as explained previously. Each method was configured so that the wires changed position 32 times along the harness length (i.e., 32 segments were used for the reasonable worst-case estimate). The harness was assumed to be 2-m long and positioned above a large return plane. Simulations were performed from 10 kHz

$$xtalk_{cap} \cong \left(\frac{Z_x}{(R_S + Z_x + j\omega L_{11})} \right) \left(\frac{[j\omega(C_x + 2C_{12}) + (C_{12}/C_{o_avg} Z_{all})]}{((1/Z_{all}) + 2j\omega C_x) (1 + (1/j\omega C_x R_{NE2} // R_{FE2}) + (C_{12}/C_x)) - j\omega C_{o_avg}} \right) \quad (5)$$

Fig. 9. Near-end crosstalk when all circuits were loaded with 50 Ω .Fig. 10. Far-end crosstalk when all circuits were loaded with 50 Ω .

to 10 MHz, where the harness could be considered electrically small. The number of wires in the harness, the height above the return plane, and the value of source and load impedances were varied, as indicated in the following test configurations:

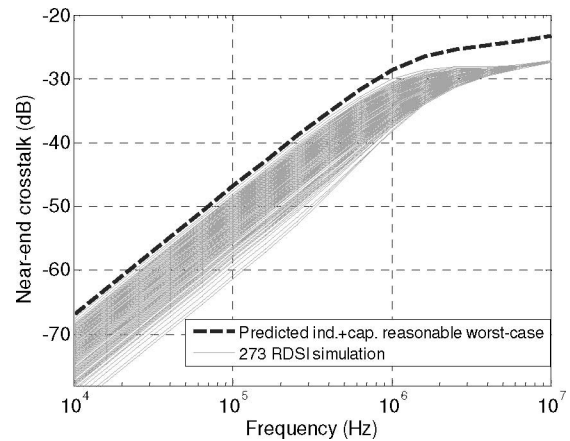
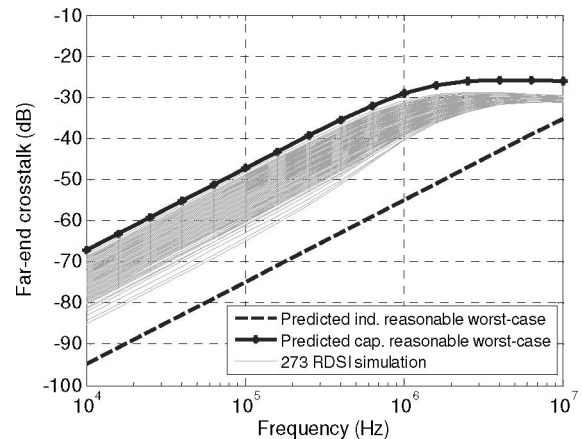
- 1) scenario 1: 3 wires, height = 2 cm, and 50- Ω and 1-k Ω terminations;
- 2) scenario 2: 14 wires, height = 2 cm, and all terminations 50 Ω ;
- 3) scenario 3: 14 wires, height = 2 cm, and all terminations 1 k Ω ;
- 4) scenario 4: 14 wires, lying on return plane, and all terminations either 50 Ω or all terminations 1 k Ω ;
- 5) scenario 5: 14 wires, lying on return plane, and terminations varied to mimic realistic harness impedances;
- 6) scenario 6: 14 wires, lying on return plane, and all terminations either 50 Ω or 1 k Ω ; presence of return wire.

A. Scenario 1: 3 Wires, Height = 2 cm, and 50- Ω and 1-k Ω Terminations

In the first scenario tested, the harness had only three wires, was 2 cm above the return plane, and was loaded on both ends with either 50- Ω loads—and inductive coupling dominated—or 1-k Ω loads—and capacitive coupling dominated. Under these configurations, the variation in crosstalk among harness instantiations is small and results should be very close to the analytic calculations. The reasonable worst-case estimate (as well as the RDSI estimate) was within 1 dB of the analytic estimate across the entire frequency range, verifying that the technique works well even for a small number of wires.

B. Scenario 2: 14 Wires, Height = 2 cm, and All Terminations 50 Ω

For this configuration, inductive coupling should dominate, since the termination impedances are relatively low. The reasonable worst-case crosstalk and the crosstalk predicted by 273 RDSI simulations of random harness instantiations are shown in Fig. 9 for the near-end crosstalk and Fig. 10 for the far-end crosstalk. The reasonable worst-case estimate is within about 5 dB of the worst crosstalk found by the RDSI algorithm.

Fig. 11. Near-end crosstalk when all circuits were loaded with 1 k Ω .Fig. 12. Far-end crosstalk when all circuits were loaded with 1 k Ω .

C. Scenario 3: 14 Wires, Height = 2 cm, and All Terminations 1 k Ω

In this scenario, capacitive coupling should dominate. The near- and far-end crosstalks are shown in Figs. 11 and 12, respectively. The reasonable worst-case estimate was within about 5 dB of the worst value found using the RDSI algorithm.

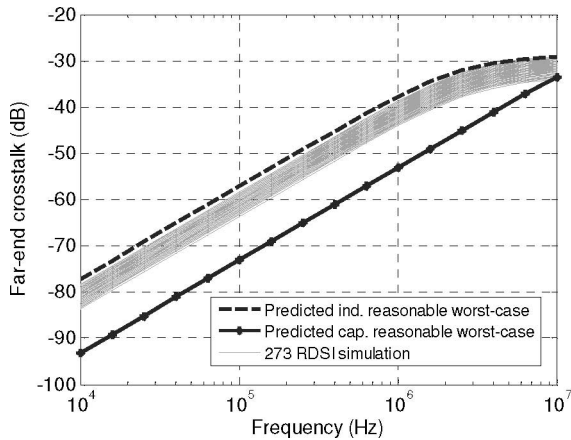


Fig. 13. Far-end crosstalk when the bundle was lying on the return plane and all circuits were loaded with 50Ω .

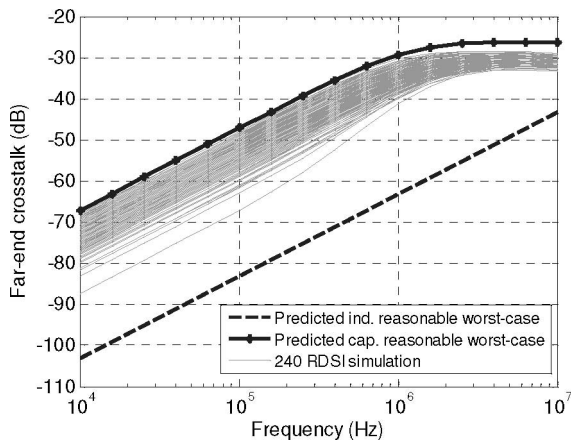


Fig. 14. Far-end crosstalk when the bundle was lying on the return plane and all circuits were loaded with $1 \text{ k}\Omega$.

D. Scenario 4: 14 Wires, Lying on Return Plane, and All Terminations Either 50Ω or $1 \text{ k}\Omega$

To study the ability to estimate reasonable worst-case crosstalk for small heights, simulations were performed with the harness lying directly on the return plane. This case is expected to be challenging for the proposed estimation method since the variation of inductive coupling should be much larger and the application of some approximations used by the estimate may not be as appropriate as when the harness is far from the return plane. Estimates of crosstalk are shown in Fig. 13 when all terminations were 50Ω and in Fig. 14 when all terminations were $1 \text{ k}\Omega$. The reasonable worst-case estimate was within a few decibels of the worst-case estimated using RDSI for both termination conditions.

E. Scenario 5: 14 Wires, Lying on Return Plane, Terminations Varied to Mimic Realistic Harness Impedances

In this case, the harness was terminated with a variety of impedances, as shown in Table I. These terminations are similar to those used by others in the study of the statistical characteristics of harness crosstalk [1], [2], [6], [7]. The first experiments

TABLE I
NEAR-END AND FAR-END LOADS

Circuit #	R_{NE}	R_{FE}	Circuit #	R_{NE}	R_{FE}
1	$2 \text{ k}\Omega$	$2 \text{ k}\Omega$	8	10Ω	$1 \text{ k}\Omega$
2	10Ω	100Ω	9	$15 \text{ k}\Omega$	10Ω
3	$100 \text{ k}\Omega$	10Ω	10	47Ω	10Ω
4	47Ω	$100 \text{ k}\Omega$	11	$1 \text{ k}\Omega$	10Ω
5	$1 \text{ k}\Omega$	47Ω	12	10Ω	$1 \text{ k}\Omega$
6	$100 \text{ k}\Omega$	$15 \text{ k}\Omega$	13	10Ω	$15 \text{ k}\Omega$
7	$15 \text{ k}\Omega$	$15 \text{ k}\Omega$	14	47Ω	47Ω

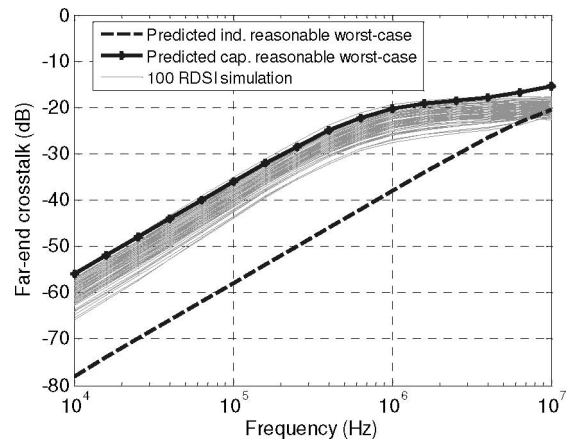


Fig. 15. Far-end crosstalk from circuit 2 to circuit 1 when the bundle was loaded as shown in Table I.

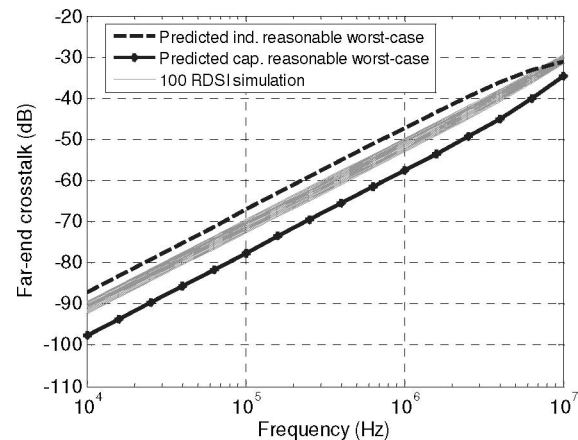


Fig. 16. Far-end crosstalk from circuit 2 to circuit 10 when the bundle was loaded as shown in Table I.

used circuit 2, with relatively small termination impedances (10 and 100Ω), as the culprit, and used circuit 1, with relatively large termination impedances ($2 \text{ k}\Omega$), and circuit 10, with relatively small impedances (47 and 10Ω), as the victims. Far-end crosstalk is shown in Fig. 15 when circuit 1 was the victim and in Fig. 16 when circuit 10 was the victim. The reasonable worst-case estimate was within about 3 dB of the worst crosstalk found using RDSI in these cases.

The second experiments used circuit 1, with a relatively large termination impedance ($2 \text{ k}\Omega$), as the culprit, and used circuit 2,

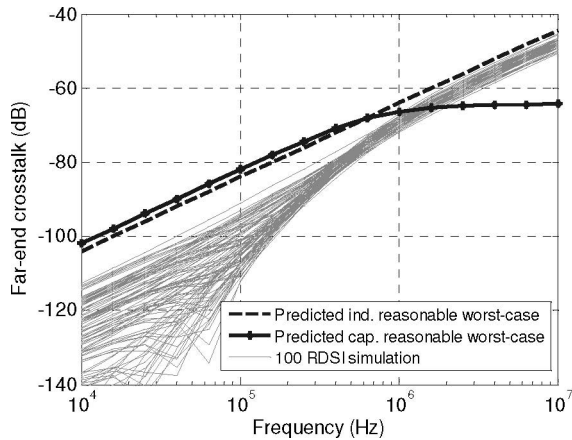


Fig. 17. Far-end crosstalk from circuit 1 to circuit 2 when the bundle was loaded as shown in Table I.

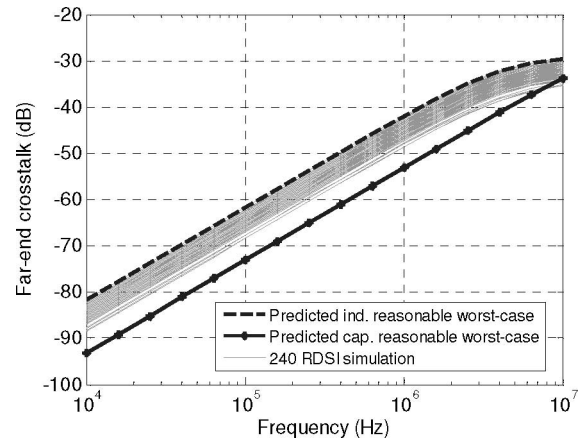


Fig. 19. Far-end crosstalk when the bundle was lying on the return plane and all wires were loaded with $50\ \Omega$ except a return wire.

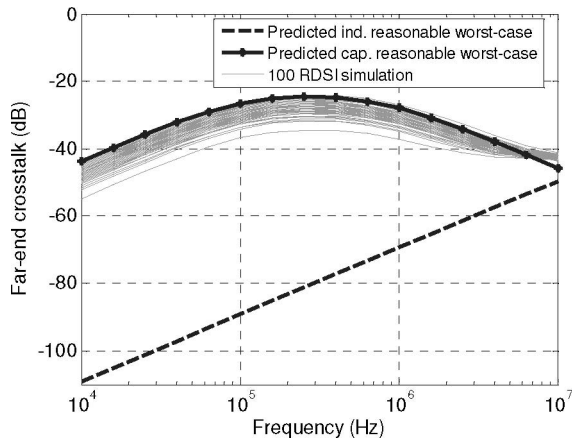


Fig. 18. Far-end crosstalk from circuit 1 to circuit 7 when the bundle was loaded as shown in Table I.

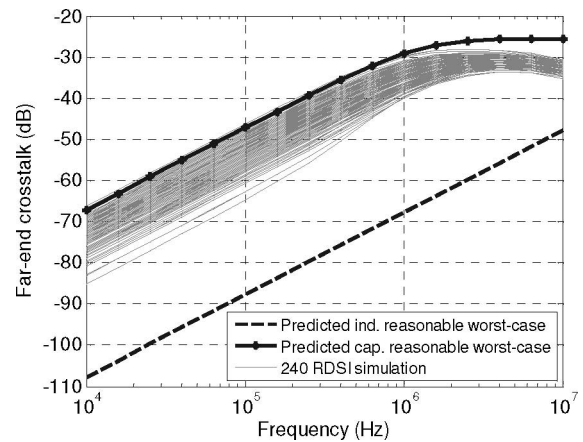


Fig. 20. Far-end crosstalk when the bundle was lying on the return plane and all wires were loaded with $1\ \text{k}\Omega$ except a return wire.

with a relatively small termination impedance (10 and $100\ \Omega$), and circuit 7, with a relatively large termination impedance ($15\ \text{k}\Omega$), as the victims. The far-end crosstalk for these configurations is shown in Figs. 17 and 18. The reasonable worst-case estimate of crosstalk to circuit 7 was within a few decibels of the worst crosstalk found by the RDSI algorithm over the frequency range studied. The reasonable worst-case overestimated the worst crosstalk to circuit 1, however, by about $10\ \text{dB}$ below $1\ \text{MHz}$. This overestimation results because neither inductive nor capacitive coupling dominates for this configuration and the two cancel each out at the far end, resulting in lower crosstalk than is found with either inductive or capacitive crosstalk alone.

F. Scenario 6: 14 Wires, Lying on Return Plane, and All Terminations Either $50\ \Omega$ or $1\ \text{k}\Omega$; Presence of Return Wire

Another case that is expected to be challenging for the proposed estimation technique is the case where a return wire exists within the harness. This case is challenging since high-frequency current will return over this wire rather than over the return plane, and some approximations may not be as appro-

priate as when currents return far from the harness. To perform this estimation, the extraction of the L and C matrices was performed such that one wire in the harness was designated as a return wire and was lumped with the return plane in the 2-D extraction tool, so the return plane and return wire were treated as the same conductor. Thus, for the harness shown in Fig. 1, the harness included 13 wires associated with circuits and 1 wire for the return, and the L and C matrices contained 13 rows and columns. Other estimation steps were performed as before. Estimated crosstalk is shown in Fig. 19 when all circuits were terminated with $50\ \Omega$ and in Fig. 20 when all circuits were terminated with $1\ \text{k}\Omega$. The reasonable worst case was within a few decibels of the worst case found with the RDSI algorithm. Simulations where the harness was $2\ \text{cm}$ above the return plane were also performed with slightly better results than when the harness was lying on the return plane.

V. DISCUSSION

The proposed method of estimating the reasonable worst-case crosstalk successfully bound the worst crosstalk found through multiple RDSI simulations within $5\ \text{dB}$ or less for all the

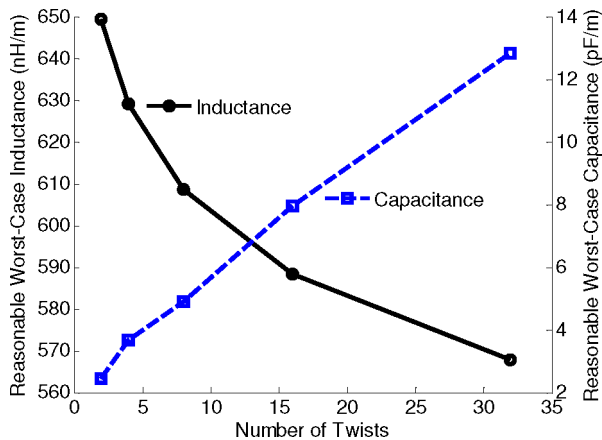


Fig. 21. Reasonable worst-case mutual inductance and capacitance as a function of wire twist.

scenarios tested except for the scenario shown in Fig. 17. While only resistive loads were explored, good results are also expected with reactive loads, since they do not make a fundamental change to the algorithm. For similar reasons, good results are also expected for larger bundle sizes or larger distances above the return plane.

The estimate of the rate that wires change within the harness has a direct impact on the estimate of the reasonable worst-case crosstalk. The rate that wires change position is modeled here by the number of segments used to estimate the probability distribution for inductance or capacitance. As shown in Figs. 3 and 5, using eight segments rather than 32 segments results in a reasonable worst-case mutual inductance of about 600 rather than 570 nH/m and a mutual capacitance of about 5 rather than 13 pF/m. This change is further illustrated in Fig. 21. Misestimating the rate that wires change position could result in a larger or smaller estimate of the reasonable worst-case crosstalk than occurs in the actual harness. From (4) and (5), the error in the estimate of crosstalk is approximately proportional to the error in the estimate of mutual inductance or capacitance. The sensitivity of estimated crosstalk to twist is then approximately proportional to the slope of the curves in Fig. 21. Crosstalk is most sensitive to twist when capacitive coupling dominates, where capacitance (and the estimate of crosstalk) changes by a factor of three when increasing the number of twists from 8 to 32 (or about 4% per twist at 16 twists). This misestimation will also occur with the RDSI or similar algorithms.

It is challenging to estimate the reasonable worst-case far-end crosstalk using the proposed method when inductive and capacitive couplings are out of phase and approximately equal in size, as occurred in Fig. 17. The current technique will overestimate crosstalk in these scenarios since it cannot accurately predict the value of both inductive and capacitive crosstalk for *specific* configurations. Accurate estimation requires formation of a joint probability distribution between inductance and capacitance so that reasonable levels of cancellation can be predicted. Development of this method is left for future work. The current method, however, can be considered a conservative estimate when in-

ductive and capacitive couplings contribute nearly equally to far-end crosstalk.

Here, we studied only the variation in the crosstalk due to the change in wire positions. In real harnesses, the height of the harness also varies randomly above the return plane as does the compactness of the harness. The proposed technique might be extended to account for these conditions by calculating L and C matrices for a representative sample of possible heights or compactness, attributing a given probability to each condition, and then using this information to calculate a probability distribution for inductance and capacitance, as shown in Figs. 3 and 4. Once these probability distributions are known, the reasonable worst-case crosstalk can be found using (4) or (5).

VI. CONCLUSION

The proposed method well estimates the reasonable worst-case crosstalk due to random variation of wire position within cable bundles. The advantage of the technique is not only an improved estimation speed, but also the potential to improve the understanding of why problems occur and how to fix them, since results are found from relatively simple closed-form approximations, and L and C matrices. Accurate prediction depends on accurate knowledge of harness parameters, like harness height or the rate that wires change position along the harness length. While random variation in harness height or other parameters were not dealt with here, the technique might also be extended to account for variations in these parameters.

REFERENCES

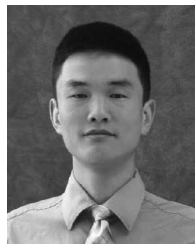
- [1] G. Capraro and C. R. Paul, "A probabilistic approach to wire coupling interference prediction," in *Proc. 1981 IEEE Int. Symp. EMC*, pp. 267–272.
- [2] C. R. Paul, "Sensitivity of crosstalk to variations in cable bundles," in *Proc. 1987 IEEE Int. Symp. EMC*, pp. 617–622.
- [3] D. G. Beetner, H. Weng, M. Wu, and T. Hubing, "Validation of worst-case and statistical models for an automotive EMC expert system," in *Proc. 2007 IEEE Int. Symp. Electromagn. Compat.*, Jul., pp. 1–5.
- [4] W. T. Smith, C. R. Paul, J. S. Savage, S. K. Das, A. D. Cooperider, and R. K. Frazier, "Crosstalk modeling for automotive harnesses," in *Proc. 1994 IEEE Int. Symp. Electromagn. Compat.*, Aug., pp. 447–452.
- [5] S. Shiran, B. Reiser, and H. Cory, "A probabilistic model for the evaluation of coupling between transmission lines," *IEEE Trans. Electromagn. Compat.*, vol. 35, no. 3, pp. 387–393, Aug. 1993.
- [6] A. Ciccolella and F. G. Canavero, "Stochastic prediction of wire coupling interference," in *Proc. 1995 IEEE Int. Symp. EMC*, pp. 51–56.
- [7] S. Sun, G. Liu, J. Drewniak, and D. Pommerenke, "Hand-assembled cable bundle modeling for crosstalk and common-mode radiation prediction," *IEEE Trans. Electromagn. Compat.*, vol. 49, no. 3, pp. 708–718, Aug. 2007.
- [8] D. Bellan and S. A. Pignari, "Estimation of crosstalk in nonuniform cable bundles," in *Proc. 2005 IEEE Int. Symp. Electromagn. Compat.*, Aug. 8–12, pp. 336–341.
- [9] M. Wu, D. Beetner, and T. Hubing, "Estimation of the statistical variation of crosstalk in wiring harnesses," in *Proc. IEEE Int. Symp. EMC*, Aug. 2008, pp. 1–7.
- [10] C. R. Paul, *Analysis of Multiconductor Transmission Lines*. Hoboken, NJ: Wiley, 1994.
- [11] A. Papoulis and S. U. Pillai, *Probability, Random Variables and Stochastic Processes With Errata Sheet*, 4th ed. New York: McGraw-Hill Higher Education, 2002.



Meilin Wu received the B.S. degree in engineering physics, and the M.S. degree in nuclear science and technology from Tsinghua University, Beijing, China, in 2004 and 2006, respectively, and a second M.S. degree in electrical engineering from the Missouri University of Science and Technology, Rolla, in 2009.

From 2006 to 2008, he was a Graduate Research Assistant in the Electromagnetic Compatibility Laboratory, Missouri University of Science and Technology. He is currently a Signal Integrity Engineer at

Amphenol-TCS, Nashua, NH. His research interests include signal integrity and electromagnetic interference problems in high-speed, high-density connectors, and backplane systems.



Haixin Ke (M'06) received the B.S.E.E. and M.S.E.E. degrees from Tsinghua University, Beijing, China, in 1998 and 2001, respectively, and the Ph.D. degree in electrical engineering from the Missouri University of Science and Technology (formerly called the University of Missouri-Rolla), Rolla, in 2006.

Since 2006, he has been a Postdoctoral Researcher at Clemson University, Clemson, SC. His current research interests include computational electromagnetics, electromagnetic compatibility, and vehicular

electronic systems.



Daryl G. Beetner (S'89–M'98–SM'03) received the B.S. degree in electrical engineering from Southern Illinois University, Edwardsville, in 1990, and the M.S. and D.Sc. degrees in electrical engineering from Washington University, St Louis, MO, in 1994 and 1997, respectively.

He is currently an Associate Professor of electrical and computer engineering at the Missouri University of Science and Technology (formerly called the University of Missouri-Rolla), Rolla, where he is also the Associate Chair of the Computer Engineering Program and is engaged in conducting research in the Electromagnetic Compatibility Laboratory on a wide variety of topics including electromagnetic compatibility at the chip and system level, and detection and neutralization of

explosive devices.



Shishuang Sun (S'03–M'07) received the B.S. and M.S. degrees in electrical engineering from Shanghai JiaoTong University, Shanghai, China, and the Ph.D. degree in electrical engineering from the Missouri University of Science and Technology (formerly known as the University of Missouri-Rolla), Rolla.

He is currently with Altera Corporation, San Jose, CA, where he is a Member of the Technical Staff in the Product Characterization Group. His research interests include signal integrity in high-speed digital systems, and power delivery network design and modeling.

systems, and power delivery network design and modeling.



Todd H. Hubing (S'82–M'82–SM'93–F'06) received the B.S.E.E. degree from the Massachusetts Institute of Technology, Cambridge, in 1980, the M.S.E.E. degree from Purdue University, West Lafayette, IN, in 1982, and the Ph.D. degree in electrical engineering from North Carolina State University, Raleigh, in 1988.

From 1982 to 1989, he was with the Electromagnetic Compatibility (EMC) Laboratory, IBM Communications Products Division, Research Triangle Park, NC. During 1989, he was a faculty member

at the University of Missouri-Rolla, where he was engaged in analyzing and developing solutions for a wide range of EMC problems affecting the electronics industry. During 2006, he was the Michelin Professor for vehicular electronics at Clemson University, Clemson, SC, where he is currently engaged in EMC and computational electromagnetic modeling, particularly, as it is applied to automotive and aerospace electronics.

Prof. Hubing is the Past President of the IEEE EMC Society, where he is currently the Vice President for Communication Services. He is a Fellow of the Applied Computational Electromagnetic Society.